



In vivo evidence for long-term vascular remodeling resulting from chronic cerebral hypoperfusion in mice

Tom Struys¹, Kristof Govaerts², Wouter Oosterlinck³,
 Cindy Casteels⁴, Annelies Bronckaers¹, Michel Koole⁴,
 Koen Van Laere⁴, Paul Herijgers³, Ivo Lambrichts¹,
 Uwe Himmelreich² and Tom Dresselaers^{2,5}

Abstract

We have characterized both acute and long-term vascular and metabolic effects of unilateral common carotid artery occlusion in mice by *in vivo* magnetic resonance imaging and positron emission tomography. This common carotid artery occlusion model induces chronic cerebral hypoperfusion and is therefore relevant to both preclinical stroke studies, where it serves as a control condition for a commonly used mouse model of ischemic stroke, and neurodegeneration, as chronic hypoperfusion is causative to cognitive decline. By using perfusion magnetic resonance imaging, we demonstrate that under isoflurane anesthesia, cerebral perfusion levels recover gradually over one month. This recovery is paralleled by an increase in lumen diameter and altered tortuosity of the contralateral internal carotid artery at one year post-ligation as derived from magnetic resonance angiography data. Under urethane/ α -chloralose anesthesia, no acute perfusion differences are observed, but the vascular response capacity to hypercapnia is found to be compromised. These hemispheric perfusion alterations are confirmed by water [¹⁵O]-H₂O positron emission tomography. Glucose metabolism ([¹⁸F]-FDG positron emission tomography) or white matter organization (diffusion-weighted magnetic resonance imaging) did not show any significant alterations. In conclusion, permanent unilateral common carotid artery occlusion results in acute and long-term vascular remodeling, which may have immediate consequences for animal models of stroke but also vascular dementia.

Keywords

Arterial spin labeling, acute stroke, animal models, CBF, positron emission tomography

Received 12 June 2015; Revised 27 November 2015; 22 January 2016; Accepted 15 February 2016

Introduction

Chronic cerebral hypoperfusion, also termed oligemia, defines the reduced cerebral blood flow (CBF) in the brain that results from a wide range of disorders which directly or indirectly affect the arterial cerebral input. Constriction or complete blockage of the blood flow in one of the main feeding arteries, as seen in carotid stenosis and stroke, can be regarded as the most common cause.^{1,2} Reduction in cardiac output resulting from coronary artery disease and/or ventricular tachycardia has also been found to markedly affect cerebral perfusion.³ Even in normal aging, cerebral perfusion is known to be reduced by 15 to 20% between the age of 20 and 65.⁴ Although this decrease does not

¹Biomedical Research Institute – Morphology Research Group, Hasselt University, Hasselt, Belgium

²Biomedical MRI Unit – MoSAIC, Department of Imaging & Pathology, KU Leuven, Leuven, Belgium

³Research Unit of Experimental Cardiac Surgery, Department of Cardiovascular Sciences, KU Leuven, Leuven, Belgium

⁴Nuclear Medicine – MoSAIC, Department of Imaging & Pathology, KU Leuven, Leuven, Belgium

⁵Radiology, University Hospitals, Leuven, Belgium

Corresponding author:

Tom Struys, Biomedical Research Institute – Morphology Research Group, Hasselt University, Belgium, Agoralaan, Building D, 3590 Diepenbeek, Belgium.
 Email: tom.struys@uhasselt.be

necessarily imply the occurrence of major functional deficits, chronic cerebral hypoperfusion has been suggested to contribute to the onset or modification of the evolution of neurodegenerative diseases such as Alzheimer's Disease (AD).⁵ Altogether, it is widely recognized that chronic hypoperfusion is involved in a wide range of neuropathologies and particularly in those relevant in aging and stroke.

Mouse models of oligemia have been developed using global permanent bilateral carotid artery stenosis⁶ or either bilateral stepwise or permanent unilateral occlusion of the common carotid artery (CCA).^{7,8} Importantly, the latter is, besides neurodegeneration, also relevant to the transient middle cerebral artery occlusion (MCAO) model, a common ischemic stroke model in rodents, where permanent unilateral ligation is performed as part of the surgical procedure. In this context, it serves as the sham operated, experimental control group in many stroke-related preclinical studies.⁹ Many of those studies have investigated the potential of stimulating angiogenesis following ischemic stroke to counteract the adverse events elicited by the compromised blood flow.^{10,11} Recent advances in high-field magnetic resonance imaging (MRI) offer the possibility of longitudinal monitoring of CBF in addition to its classical application of anatomical characterization of focal ischemic lesions.¹² Although studies are using perfusion MRI to compare CBF between experimental groups in a longitudinal way,¹³ in-depth knowledge about the acute and long-term effect of a permanent unilateral CCA ligation on cerebral perfusion is still lacking. Such work would also pave the way for further investigation of the molecular mechanisms related to oxygen sensors¹⁴ or neurodegeneration^{15,16} using transgenic and knockout animals.

In this study, we report on arterial spin labeling (ASL) MRI to monitor longitudinal CBF changes and hemispheric variations observed in mice after permanent unilateral CCA ligation. The hemispheric perfusion differences were also investigated using [¹⁵O]-H₂O positron emission tomography (PET). Although basal perfusion differences can be an effective disease marker, the change in CBF values in response to stimuli such as hypercapnia, also known as cerebral vascular response (CVR), may be an even more sensitive indicator. Since it was recently shown that under ventilation the CVR can also be determined under continuous monitoring of expired CO₂ levels,¹⁷ we implemented this approach in our study. These readouts of cerebral perfusion were linked to the lumen diameter and tortuosity of the internal carotid arteries derived from MR angiography data. Furthermore, metabolic effects from chronic unilateral CCA occlusion were assessed using [¹⁸F]-fluoro-deoxy-dglucose (FDG) PET. Finally, the presence of ischemic lesions or long-term white matter

degradation resulting from permanent unilateral CCA ligation was investigated using diffusion-weighted MRI. We conclude that the acute decrease in CBF seen after permanent unilateral CCA occlusion shows spontaneous long-term recovery and that this process is paralleled by variations in the diameter of the ipsi- and contralateral internal carotid artery but without metabolic or white matter alterations.

Materials and methods

Preliminary experiments

To determine which methodology would allow an assessment of the vascular response in mice using ASL MRI, we first performed a set of experiments in C57J/BL6 mice (± 9 weeks old, male) under different conditions: (a) free breathing inhalation of 5% CO₂/95% O₂ under isoflurane versus 100% O₂ (n=6), (b) ventilated inhalation of 5% CO₂/95% O₂ under isoflurane versus 100% O₂ (n=8) and compared those results to our previous work using hypoventilation under urethane/alpha-chloralose.¹⁷ Other experimental details are as described below.

Main experiments

Animals. In this study, male C57J/BL6 mice (two months of age; 25–30 g body weight; Harlan, Germany) were used (numbers are mentioned for the different experiments). Prior to surgery, the animals were housed in groups of five in a temperature and humidity-controlled environment on a 12/12-h light/dark cycle with free access to standard rodent food and water. In total, 72 animals were used in this study. Animals were randomly assigned to groups, but operators were not blinded to the study. All experiments described in this study were performed according to institutional guidelines and compliant with national and international laws and policies governing the use of animals in biomedical research. The Animal Research Committee of the catholic university of Leuven, Belgium approved the study protocol (protocol number 102/2011). During the study, all efforts were made to minimize animal distress and the number of animals used. The animal experiments were reported on according the ARRIVE guidelines.

Surgery: Permanent unilateral CCA ligation. Anesthesia was induced through inhalation of pure oxygen enriched with 2% isoflurane. Rectal temperature was monitored during surgery and until recovery from anesthesia and maintained at 37°C using a heating blanket. Chronic hypoperfusion was induced by a permanent unilateral ligation of the CCA. Briefly, after a ventral midline

incision in the neck region, the left CCA was carefully separated from the adjacent vagus nerve and permanently ligated with a 6-0 silk suture. All animals survived surgery.

Experimental design

For imaging studies, free breathing or ventilated animals were placed on an animal bed (Bruker Biospin, Ettlingen, Germany) and physiologically monitored for heart rate, body temperature and respiratory rate. Rectal temperature was kept in the range of $37 \pm 1^\circ\text{C}$ using a controlled warm water circuit (MRI) or electrical heating pad (PET). Detailed physiological parameters are listed in supplementary Table 1.

Free breathing. Mice were anesthetized using isoflurane anesthesia under free breathing conditions (1.8% isoflurane for induction; $1.4 \pm 0.2\%$ for maintenance – both in pure oxygen).

Sub-groups of animals were scanned at different time points post ligation (1, 7, 14, 30 days and 1 year; $n = 34, 9, 9, 8$ and 11 , respectively, non-ligated: $n = 9$). MR angiography was recorded at 1, 14, 30 days and 1 year: $n = 13, 6, 6, 10$, respectively. Non-operated mice were also included ($n = 7$ with 3 months old $n = 4$ and 1 year old $n = 3$; pooled since no significant differences and minimal variation in all parameters was observed).

Ventilated. Procedures were described previously¹⁷ with some modifications as listed below. Anesthesia was induced through intraperitoneal (i.p.) injection of urethane (1.2 g/kg) and α -chloralose (50 mg/kg). Mice were placed in a supine position on a heating pad, and rectal temperature was kept at $37^\circ\text{C} \pm 1^\circ\text{C}$. Atropine (0.05 mg/kg) and pancuronium (0.16 mg/kg) were administered i.p. to reduce saliva production, facilitate the intubation and induce muscle relaxation. Endotracheal intubation was performed under direct vision with a 24 G tube over a guide-wire (Insyte-W, Becton Dickinson, New Jersey, USA). Ventilation occurred under a gas mixture of oxygen in air (ratio: 1:2; resulting in a mixture containing mainly 47% O_2 , 52% N_2 , 0.5% Ar, 0.02% CO_2) with continuous monitoring of expired CO_2 (Vaisala CarboCap[®] Carbon dioxide transmitters series, GMM221, Bonn, Germany). Considering the tubing length and dead space surrounding the detector, the measured CO_2 concentration shows an equilibrium concentration that is obtained in a calibrated volume surrounding the detector and not an end tidal pCO_2 .

For ventilated animals, the experimental protocol consisted of a stabilization period under normoventilation followed by a hypercapnic challenge through hypoventilation and a return to baseline settings.

Ventilation was started at a tidal volume (TV) of $3 \times \text{body weight (g)} + 155 \mu\text{l}$ and a respiratory rate of 135 strokes per minute (spm) with minor individual adjustments according to the expired CO_2 levels. During hypoventilation the tidal volume (TV) was reduced by 25% and the respiratory rate was set at 70 strokes per minute (spm) for about 20 min. One perfusion map was obtained for each condition, i.e. during normocapnia or hypercapnia allowing 5 min to reach stable expired CO_2 values after onset of hypoventilation. Separate groups of animals were scanned at different time points post ligation (1, 14 and 30 days; $n = 5$ each, plus five non-operated mice) and sacrificed at the end of each scan session as required by the animal ethics guidelines of our institute.

MRI scans

MR images were acquired using a 9.4 T Biospec small animal MR system (Bruker Biospin) equipped with a 117 mm inner diameter actively shielded gradient set of 600 mT m^{-1} using a 7 cm linearly polarized resonator for transmission and an actively decoupled dedicated mouse brain surface receiver coil (Rapid Biomedical, Rimpfing, Germany). To confirm the ligation at all evaluated time points, MR angiography was used (repetition time (TR) 20 ms, echo time (TE) 2.4 ms, flip angle (FA) 20 deg, bandwidth 98 kHz, field of view (FOV) $2.56 \times 2.56 \times 1.60 \text{ cm}$, matrix $256 \times 256 \times 160$ zero-filled to $512 \times 512 \times 320$ resulting in an isotropic resolution of $50 \mu\text{m}$). Perfusion maps were recorded from a single 1 mm thick axial midbrain slice covering the thalamus, cortex and hippocampus using a flow-sensitive alternating inversion recovery (FAIR) approach^{18,19} and a rapid acquisition with relaxation enhancement (RARE) readout using the following specific parameters: TR 18 s, TE 5.2 ms, RARE factor 72, FOV $2.5 \times 2.5 \text{ cm}$, matrix 128×128 with partial Fourier acceleration to 128×72 , 10 inversion times from 300 to 3000 ms and using an inversion hyperbolic secant pulse of 14 ms with a slab thickness of 1.6 mm. At 1, 7 and 30 days post ligation, apparent diffusion coefficient (ADC) values from the same slice were determined using five b-values (0, 250, 500, 1000 and 1400 s/mm^2), a gradient echo readout and following parameters: TR 3000 ms, TE 25.3 ms, diffusion gradient duration 6 ms, separation 11 ms, two A0 images, direction $(x,y,z) = (1,1,1)$ and FOV $2.5 \times 2.5 \text{ cm}$. The ratio of the ADC to the same hemisphere in control animals is reported. At one year post ligation, fractional anisotropy (FA) and mean diffusivity (MD) were determined using a two-dimensional single shot echo planar spin echo acquisition with the following specific parameters: 13 slices of 0.6 mm thick with 0.12 mm gap, TR/TE = 7000/52 ms, acquisition matrix 128×128 zero filled to

256 × 256 resulting in a spatial resolution of 98 × 98 μm, effective bandwidth of 500 kHz, fat suppression and diffusion parameters: $\delta/\Delta = 6/14$ ms, 15 non-co-linear directions, 11 b-values (10, 20, 35, 50, 75, 100, 250, 500, 500, 750, 1000, 1250), and 3 b0 images.

MR images were processed using the Paravision 5.1 software (Bruker Biospin). Absolute CBF values were calculated using the T_1 difference method and assuming an arterial T_1 of 2.4 s.²⁰ To exclude the effect of variations in isoflurane levels (well-known vasodilator), ipsi- vs. contralateral ratios were calculated. CVR values were calculated by subtraction of the regional CBF values during normoventilation from those during hypoventilation and normalization to the increase in expired CO_2 levels (as on average observed during each perfusion scan). Since the expired CO_2 levels are measured almost 2 m away from the mouse (sensor connected to outflow of the ventilator) we report the CVR in arbitrary units (a.u.). MR angiograms were analyzed using the following procedures. After bias field correction,²¹ essential to correct for the sensitivity profile of the surface coil, blood vessels were automatically segmented in Mevislab (Mevis Medical Solutions, Bremen, Germany) using a combination of an intensity threshold and a gradient magnitude threshold; subsequently, a vessel skeleton was obtained using homotopic thinning. For analysis of the internal carotid artery (ICA), two seed points were placed: the first at the point where the carotid artery splits into the external and internal carotid arteries, and the second at the origin of the anterior cerebral artery, e.g. where both ICAs join. Then, using a shortest path algorithm, vessels were tracked between the two seed points, after which the mean erosion distance (or vessel diameter), vessel length and vessel tortuosity were calculated for the tracked blood vessel. Total vessel length was calculated by taking the sum of distances between subsequent points on the vessel path. Tortuosity was calculated using the distance metric,²² which is the ratio of the total vessel length to the linear distance between the two seed points (i.e. start and end point of the analysed vessel segment).

The dataset for the free breathing MRI perfusion scans consisted of: 18 mice scanned only on day 1, 6 animals scanned on days 1 and 7, 3 mice scanned on days 1, 7 and 30, 4 mice scanned on days 1 and 14, 2 mice scanned on days 1 and 30, 3 mice scanned on days 1, 14 and 30, 11 mice scanned at 1 year. In addition, seven control animals were scanned. Considering this mixed dataset all time points were evaluated as separate groups. The diffusion imaging was performed in the same free breathing (isoflurane) scan session as the perfusion imaging but in only a subset of animals; similar for the MR angiography (see supplementary Table 2 for details). In animals

reserved for PET analysis, ligation was confirmed by acquiring perfusion maps (at 3 to 6 h post surgery). The MR perfusion information for animals of the PET study was, however, not included in the MRI data analysis. Ligation was successful in all animals (i.e. asymmetric perfusion ipsi- vs. contralateral).

PET scans. Functional images of regional blood flow and glucose metabolism were obtained using the radioligand [^{15}O]- H_2O and [^{18}F]FDG. The synthesis of [^{15}O]- H_2O was performed according to the procedure by Fox et al.,²³ while [^{18}F]FDG was prepared by using an IBA (Ion Beam Applications, Louvain-la-Neuve, Belgium) [^{18}F]FDG synthesis module.

Before being imaged, mice were anesthetized with an intraperitoneal injection of a ketamine (75 mg/kg i.p., Ketalar®, Pfizer, Belgium) – medetomidine mixture (1.0 mg/kg, Dormitor®, Pfizer). On average 35.8 ± 7.9 MBq of [^{15}O]- H_2O and 8.9 ± 0.9 MBq of [^{18}F]FDG (specific activity range: 100–760 GBq/μmol) was injected into the tail vein using an infusion needle set. The radioligands were diluted with saline to obtain a 5% ethanol solution and injected in a total volume of approximately 300 μL. Body temperatures were maintained at $37^\circ\text{C} \pm 1^\circ\text{C}$ with a heating pad during acquisition. [^{15}O]- H_2O measurements were acquired dynamically for 2 min. After overnight fasting, [^{18}F]FDG acquisitions were done for 10 min, starting 1 h post injection. Three mice died during the [^{15}O]- H_2O PET scan session at day 1 (animals excluded from study).

Small-animal PET imaging was performed using an LSO detector-based FOCUS 220 tomograph (Siemens/Concorde Microsystems, Knoxville, TN), which has a transaxial resolution of 1.35 mm full-width at half-maximum (FWHM). Data were acquired in $256 \times 256 \times 95$ matrix with a pixel width of 0.316 mm and a slice thickness of 0.796 mm. Sinograms were reconstructed using an iterative maximum a posteriori probability algorithm with ordered subsets (MAP; 18 iterations, 9 subsets, fixed resolution: 1.5 mm).

For analysis purpose, individual [^{15}O]- H_2O and [^{18}F]FDG PET images were normalized to custom-made, ligand-specific mouse templates in Paxinos stereotactic space, allowing use of a pre-defined VOI map. Quantitative values were generated for the cerebral cortex, hippocampus and thalamus using PMODv.3.1 (PMOD Inc, Zurich, Switzerland). For [^{15}O]- H_2O and [^{18}F]FDG impairment, the affected-to-non-affected side ratio was obtained.

Immunostaining blood vessels

At one month after permanent unilateral CCA ligation, five mice were sacrificed with an i.p. injection of pentobarbital followed by a transcardial perfusion with 4%

paraformaldehyde (PFA) in phosphate-buffered saline (PBS). The brain was removed, preserved in 4% PFA in PBS, then put through a dehydrating series of graded concentrations of alcohol, and finally embedded in paraffin. Paraffin sections (5–8 μm) were made and mounted on Superfrost+ glass slides (Menzel, Braunschweig, Germany). Sections were deparaffinized with xylol, followed by decreasing concentrations of alcohol, and then washed in PBS. Prior to immunohistochemical staining, antigen retrieval was performed (sections were microwaved in a 10 mM citrate buffer at pH 6.0), and endogenous peroxidase activity was quenched with 0.5% H_2O_2 . Non-specific binding sites were blocked with 3% normal goat serum. Subsequently, sections were incubated with a rabbit anti- α -SMA polyclonal antibody (Abcam Inc., Cambridge, UK) at a dilution of 1/100 in PBS for 1 h. Next, sections were incubated with a peroxidase-labeled polymer conjugated to a goat anti-rabbit secondary antibody for 30 min (Envision System[®], DakoCytomation, Glostrup, Denmark). Immunoreactivity was visualized with 3,3'-diaminobenzidine. Sections were counterstained with Mayer's hematoxylin, coverslipped and examined using a Mirax Desk digital microscope (Zeiss, Oberkochen, Germany).

Statistical analysis

Data were confirmed to be normally distributed by a Shapiro Wilkison W test (Statistica 7.0, StatSoft, Tulsa, USA).

Ipsi- to contralateral ratios of CBF, ICA diameter or tortuosity were analyzed using a one-way ANOVA (Prism 5.04, GraphPad Soft., La Jolla, CA, USA) with Bonferroni correction for multiple comparison. When both hemispheric values at each time point and changes of hemispheric levels versus time (or controls) were analyzed, paired t-tests (L vs. R) or unpaired test (vs. time or controls) were performed with Bonferroni's correction for the number of t-tests applied (for more details see supplementary Table 2). Significance levels α correspond to: * = 0.05, ** = 0.01, *** = 0.001, **** = 0.0001, ns = not significant. Figures show average values with standard deviation (SD).

Results

Perfusion maps were recorded under free breathing conditions (isoflurane anesthesia) at different time points post-surgery (1, 7, 14, 30 days and 1 year) and compared to non-operated controls (Figure 1(a) and (b) and supplementary Figure 1). From these data, a significant trend towards normalization of absolute CBF values over time could be extracted. Average

CBF ratios between ipsi- vs. contralateral hemispheres were found to be $-45.1 \pm 8.3\%$ (day 1; n=34), $-31.6 \pm 6.2\%$ (day 7; n=9), $-22.5 \pm 5.1\%$ (day 14; n=9), $-11.7 \pm 5.0\%$ (day 30; n=8) and $-5.1 \pm 4.9\%$ (1 year; n=11) (Figure 1(b)). The perfusion reduction showed a similar level and time dependency for all three brain regions (cortex, hippocampus and thalamus) with the largest initial reduction found in the hippocampus (-50.9%).

Evaluation of the observed hemispheric CBF ratios was also investigated using [^{15}O]- H_2O -PET at two time points (day 1; n=8 and day 30; n=6) albeit under Ketamine/Domitor anesthesia. For the cortex and hippocampus, significant differences were found between 1 and 30 days following CCA ligation (supplementary Figure 2), although changes to the acute and chronic hemispheric flow ratios were less pronounced compared to the ASL-CBF measurements under isoflurane anesthesia.

The hemispheric flow differences as seen under free breathing conditions were not observed for the ASL-derived perfusion levels under urethane/ α -chloralose anesthesia in ventilated mice. None of the regions showed significant hemispheric flow differences under basal ventilation (Figure 2(a)), although a similar trend is noticeable in the acute phase (1 day post CCA ligation).

To determine if perfusion differences would become (more) apparent during a hypercapnic challenge, we first tested the possibility of inducing a hypercapnic challenge by free breathing in a 5% $\text{CO}_2/95\% \text{O}_2$ gas mixture (non-operated mice), a commonly used hypercapnic challenge in rats. Such a challenge of free breathing 5% CO_2 did not elicit an increase in CBF under isoflurane anesthesia (Thal CBF increase: $3.1 \pm 3.1\%$ vs. baseline), further confirmed by a very limited increase in arterial pCO_2 ($39.7 \pm 6.2 \text{ mmHg}$ and $43.8 \pm 5.2 \text{ mmHg}$ for 100% O_2 and 5% $\text{CO}_2/95\% \text{O}_2$, respectively). The vascular response did recovery partially when exposing the mice to hypoventilation under isoflurane (Thal CBF increase: $13.8 \pm 20.2\%$ vs. baseline; exp CO_2 : 200 ± 20 to $300 \pm 50 \text{ a.u.}$ or approximately 30 to 48 mmHg as recalculated according to literature.¹⁷ These values are still abrogated compared to the CBF increases observed under urethane/ α -chloralose anesthesia as previously reported (Thal CBF increase: $128 \pm 63\%$; ap CO_2 : $34.5 \pm \text{mmHg}$ to $64 \pm 15 \text{ mmHg}$). This preliminary data prompted us to rely on a hypoventilation challenge under urethane/ α -chloralose anesthesia to quantify differences in vascular response.

When the ventilated animals were exposed to a hypercapnic challenge resulting from a hypoventilation procedure, the hemispheric perfusion differences became apparent again (Figure 2(b)). In the acute

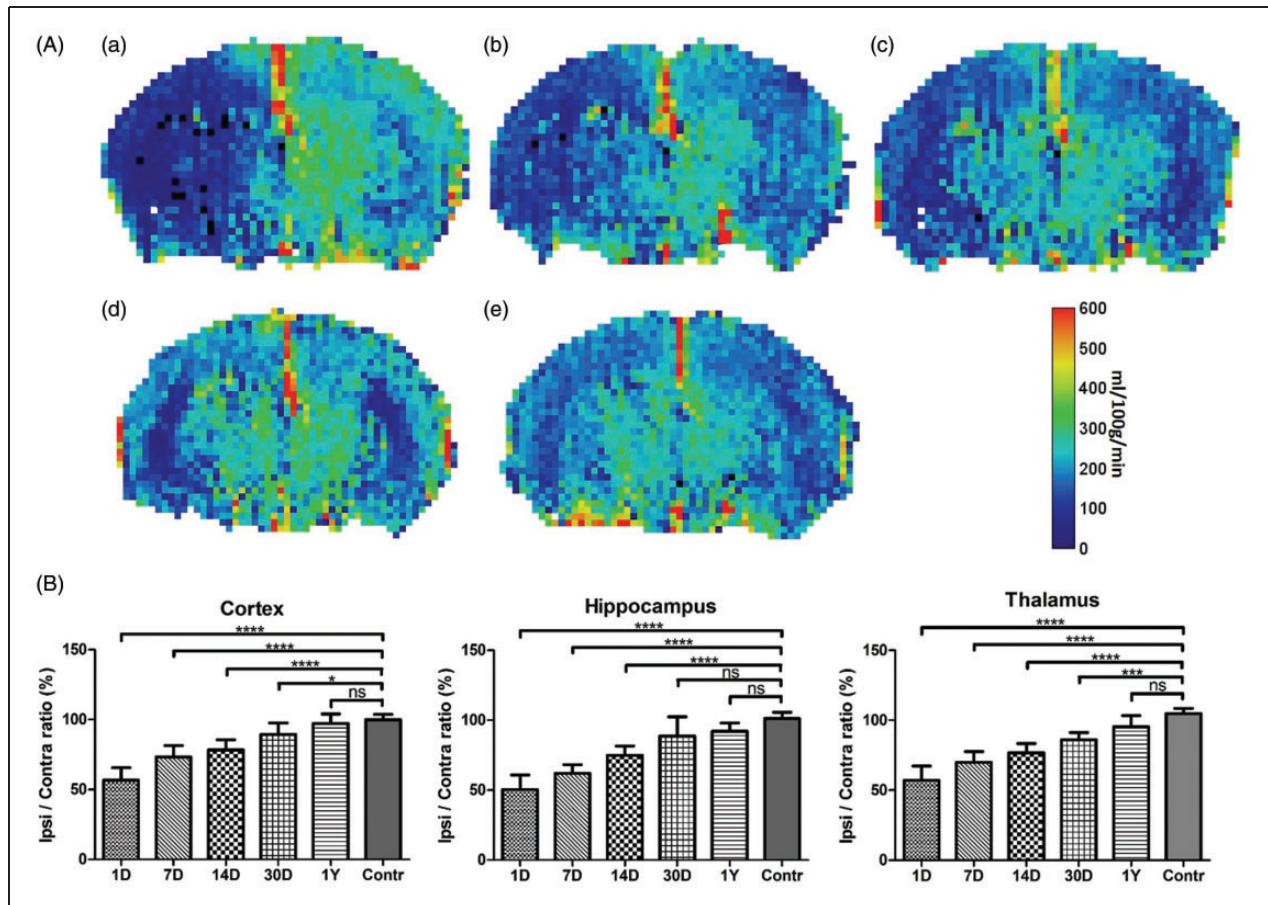


Figure 1. (a) Representative perfusion maps (separate groups) at different time points post ligation and obtained during free-breathing and isoflurane anesthesia (A = 1 day; B = 7 days; C = 30 days; D = 1 year; E = non-ligated animal). A decrease in the ipsi-lateral flow is evident in the early phase with gradual recovery over time. Color bar corresponds to a range of 0–600 ml/100g/min. (b) Ratio between the cerebral blood flow (CBF) level in the ipsi- vs. contralateral side calculated from arterial spin labeling (ASL)-based perfusion maps at different time points (1, 7, 14, 30 days and 1 year) following permanent unilateral ligation of the common carotid artery (CCA). Over 1 year, a gradual recovery of the initial hemispheric perfusion imbalance is observed under isoflurane anesthesia and free breathing conditions. (average \pm SD shown; significance indicated vs. control, i.e. non-operated mice). For precise animal numbers, please refer to supplemental Table 2.

phase, a significant drop in CVR was found in the cortex, hippocampus and thalamus region. This CVR was partially restored between 14 and 30 days following CCA ligation. For the hippocampus, the ipsi- versus contralateral CVR imbalance persisted until 30 days after CCA ligation.

Monitoring of physiological parameters showed almost equal respiration rates for free breathing mice under isoflurane anesthesia as for normoventilation conditions and a similar body temperature (see supplementary Table 1). The heart rate was lower under about 1.4% isoflurane anesthesia than under urethane/ α -chloralose anesthesia (about 460 vs. 570 bpm, respectively; see supplementary Table 1). During PET studies, heart rates were considerably lower (about 300 bpm) but mice had higher respiration rates under these

conditions (about 185 bpm). Based on the expired CO_2 values, the level of normo- and hypercapnia during the ventilation experiments was also reproducible (about 200 and 320 a.u. during normo- and hypoventilation, respectively (see supplementary Table 1). We also performed *in vivo* MR angiography to confirm the successful and permanent ligation and to investigate short- and long-term vascular remodeling. The left CCA was largely lacking in the MR angiograms at all investigated time points (representative animal in Figure 3). In addition, the MR angiograms were used to identify substantial arterial changes potentially induced by long-term oligemia as was recently reported after bilateral CCA occlusion in rats²⁴ or bilateral stenosis in mice.²⁵ In the acute phase (1 day), the ipsilateral ICA was reduced in diameter versus the contralateral

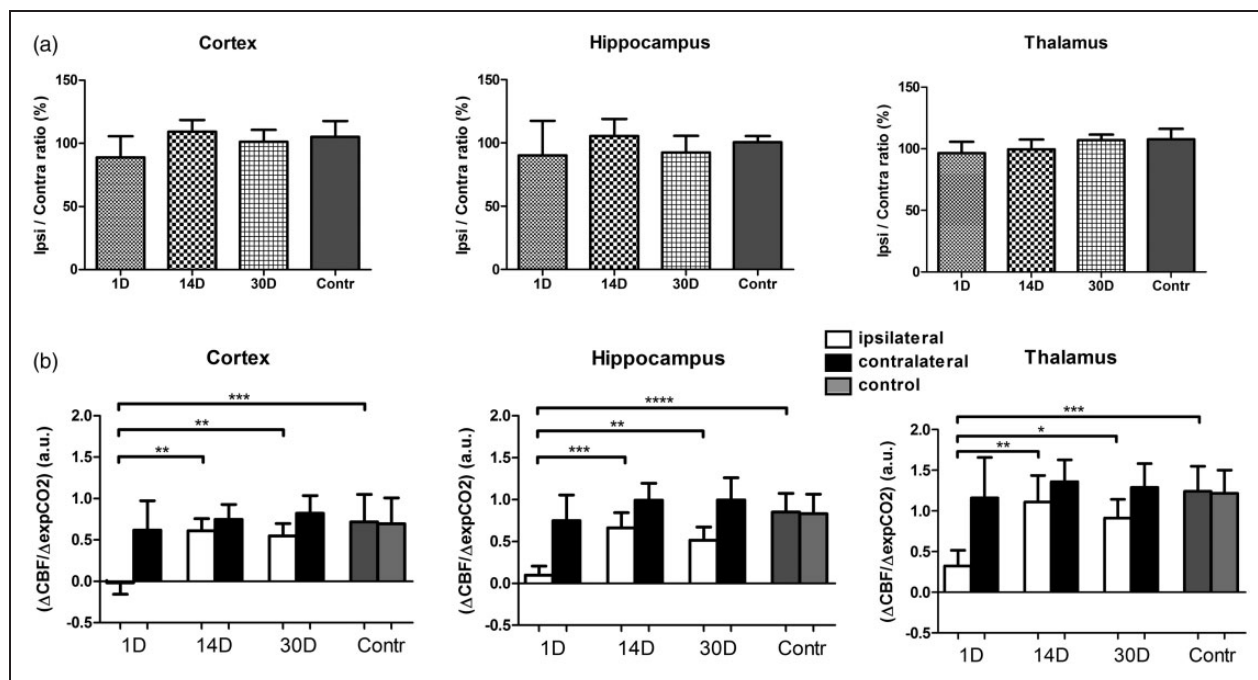


Figure 2. (a) CBF ratio ipsi vs. contralateral hemisphere as calculated from ASL-based perfusion maps at different time points (1, 14 and 30 days) following permanent unilateral ligation of the CCA. No statistically significant difference in the perfusion ratio were observed (vs. control) in ventilated mice anesthetized with urethane/ α -chloralose. (b) Cerebrovascular response (CVR) after unilateral CCA ligation. For all examined brain regions, CVR was significantly reduced at 1 day post CCA ligation compared to control animals (average \pm SD shown). For precise animal numbers, please refer to supplemental Table 2.

ICA (Figure 4(a)). At one year, the tortuosity in the contralateral ICA was increased (vs. ipsilateral ICA; Figure 4(a)). A similar trend was seen one day after CCA occlusion but this difference was not significant after Bonferroni correction for multiple comparison. Compared to non-operated controls, the tortuosity at the one year time point was also significantly increased for the contralateral side pointing towards long-term vascular changes even though blood flow was fully normalized. Similar conclusions on the acute and long-term vascular changes are obtained when performing an analysis of the ipsi vs. contralateral side (Figure 4(b)). From these data, we conclude that lumen sizes in the Circle of Willis will adjust over time to fully compensate for the acute drop in perfusion, however, with long-term impact on vessel tortuosity.

To exclude any adverse influence of the CCA ligation on brain metabolism, additional FDG-PET measurements were performed at day 1 ($n=5$) and day 30 ($n=5$) after surgery. The unilateral CCA ligation did not alter the hemispheric FDG uptake significantly (ketamine/domitor anesthesia; percentile ratio ipsi- to contralateral at 1 day: 99.2 ± 4.7 , 97.2 ± 3.3 and 97.8 ± 2.4 and at 30 days 99.2 ± 2.2 , 95.7 ± 2.6 and 98.7 ± 4.4 for cortex, hippocampus and thalamus, respectively; supplementary Figure 3).

Since white matter alterations were previously reported in a two-vessel stenosis model²⁶ and after unilateral CCA occlusion²⁷ 30 days following surgery, we also determined the diffusion characteristics (ADC, MD, FA) following CCA ligation to assess possible early and long-term white matter changes induced by a permanent unilateral CCA ligation. At day 1 or 14, no significant ADC changes were found to be present in the examined brain regions (Figure 5(a)). At one year following CCA ligation, white matter structures such as the external capsule, corpus callosum, hippocampus and thalamus together with cortical regions did not show any significant differences between ligated and normal hemispheres in mean diffusivity or fractional anisotropy, both measures of fiber bundle integrity, (Figure 5(b)). Histological validation with Kluwer-Barrera staining confirmed these findings (data not shown).

To investigate the involvement of angiogenesis in the gradual recovery of the cerebral perfusion levels, we also quantified the amount of α -SMA positive blood vessels in the different brain regions at one month (Figure 6). No significant differences were found, but for the hippocampus and thalamus regions, a trend towards a higher density of α -SMA positive blood vessels was observed.

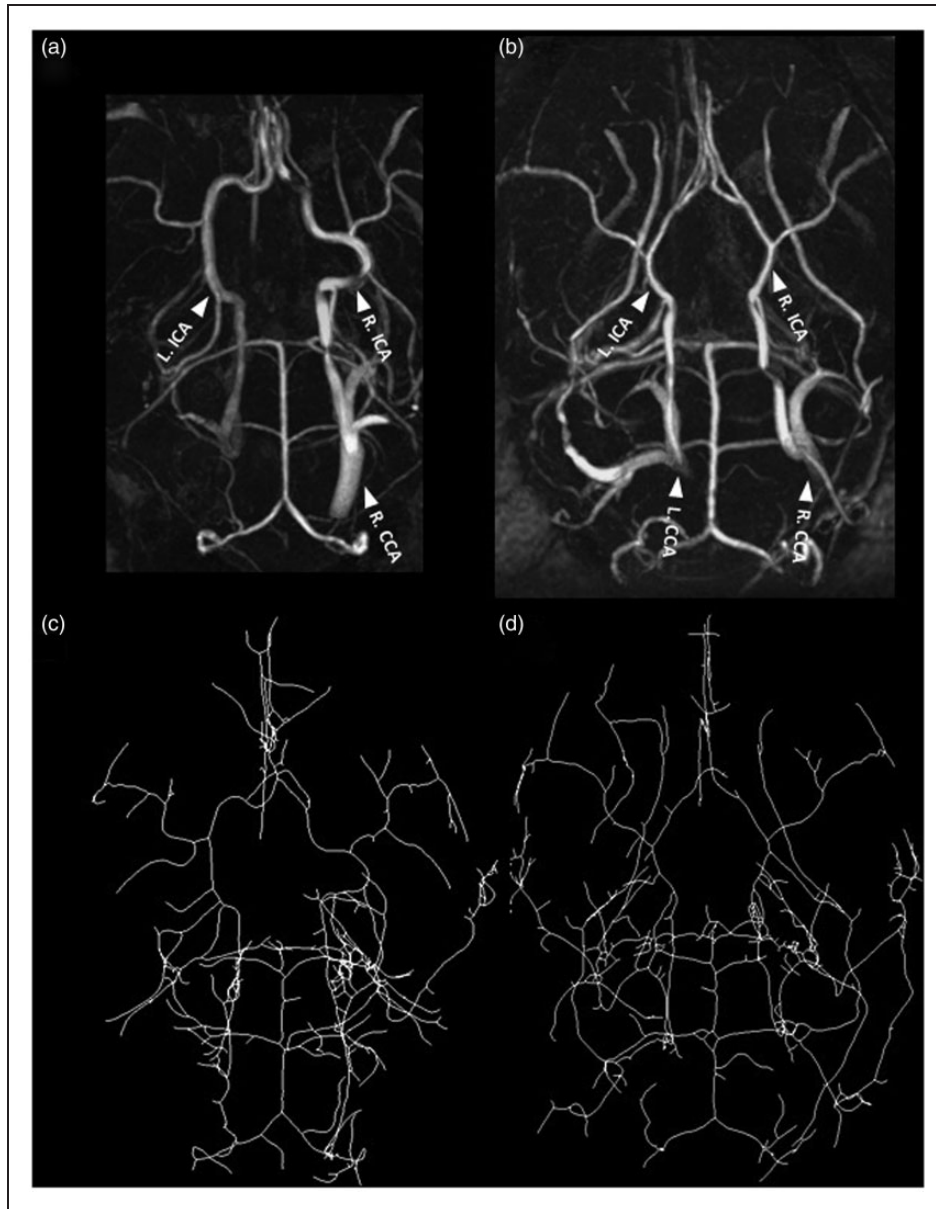


Figure 3. MR angiography: top row represents maximum intensity projections (MIP) of a one-year-old ligated mouse (a) and non-ligated mouse (b) and the vessel skeleton (c/d, ligated/non-ligated, respectively) as derived using an in-house developed pipeline using the Mevislab software (see methods for details). The left CCA is not visible thereby confirming the permanent ligation (a). At 1 year, the tortuosity of the ICA is affected. Arrows indicate: ICA = internal carotid artery and CCA = common carotid artery. For precise animal numbers, please refer to supplemental Table 2.

Discussion

Despite its clinical importance, the pathophysiological consequence of chronic hypoperfusion on the brain is still poorly understood. Animal models are crucial to unravel the impact of mild chronic hypoperfusion, and to study both compensatory mechanisms or long-term neurodegenerative effects and their potential treatments. They are also frequently used to study stroke

development and to evaluate treatment methods that focus on the restoration of CBF by means of stimulation of angiogenesis.^{10,11} This study focused on the identification of *in vivo* imaging measures for the evaluation of acute and long-term alterations resulting from permanent unilateral CCA occlusion, a model with relevance to both (vascular) dementia and stroke. We show that different MRI and PET methods can detect changes in the CBF resulting from mild hypoperfusion.

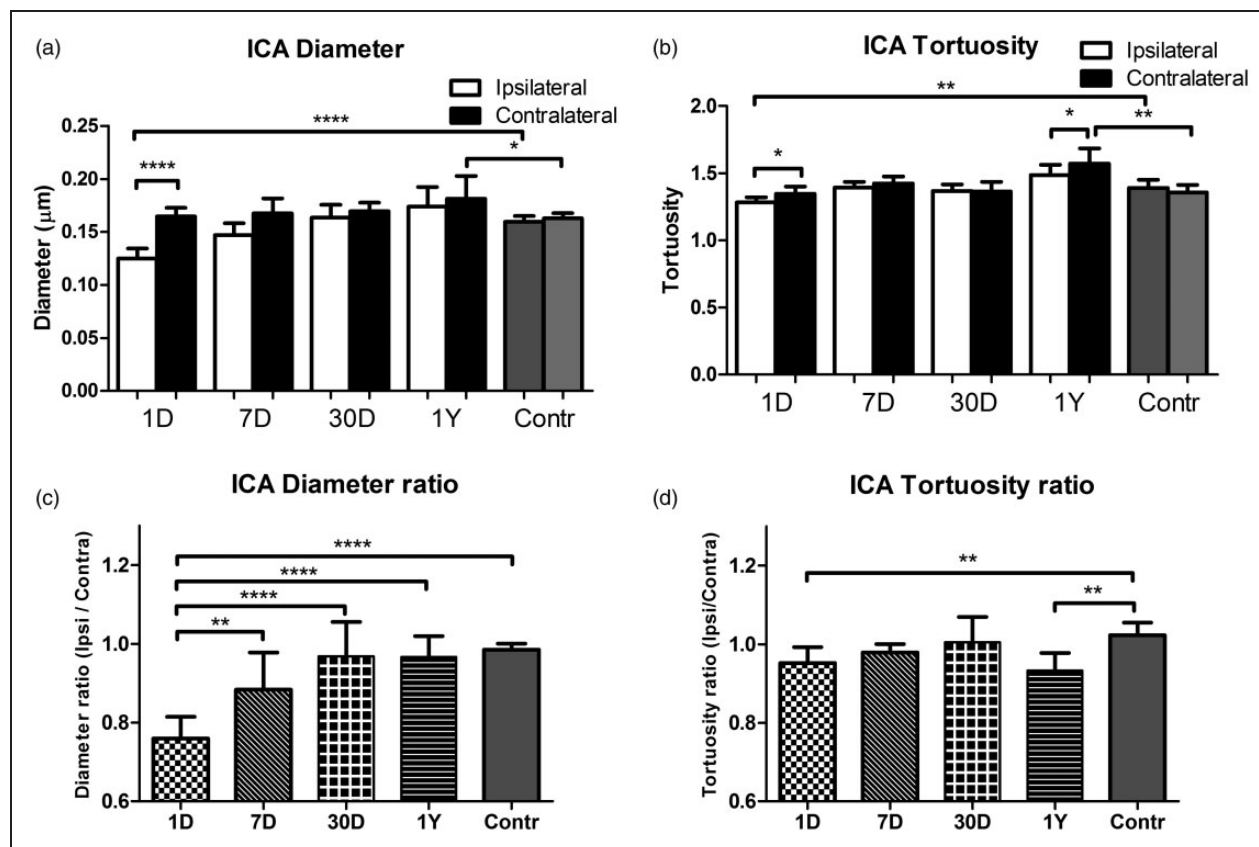


Figure 4. (a) The diameter and tortuosity index of the internal carotid arteries for the ipsilateral versus the contralateral side derived from the *in vivo* MR angiogram at different time points post permanent unilateral CCA ligation. Over time, the vessel diameter restores within approximately 1 month. At one year, the vessel tortuosity is affected without hemispheric differences in diameter (average \pm SD shown). (b) The ratio of the ipsi- to contralateral ICA diameter shows gradual recovery over time. The ratio of the ipsi- to contralateral tortuosity index is significantly different a day 1 and after one year following CCA ligation (vs. control) (average \pm SD shown). For precise animal numbers, please refer to supplemental Table 2.

However, the type of anesthesia used for these *in vivo* observations is crucial and should be considered when interpreting these data.

In this study, the effect of a permanent unilateral CCA ligation on cerebral perfusion parameters was assessed by acquiring pASL-based perfusion maps at different time points post-surgery and under two different types of anesthesia.

Perfusion results obtained under isoflurane anesthesia and under free breathing conditions showed an initial drop in the ipsi- vs. contralateral CBF of about 50% with gradual recovery over a one month period. One year post ligation, no significant differences were observable, although CBF levels still tended to be asymmetric. Similar CBF drops after unilateral CCA ligation were reported using laser Doppler flowmetry albeit with considerable variability: 35% using isoflurane anesthesia²⁷ and 40–70% using halothane anesthesia.⁸ The ASL approach used in this study markedly improved the variability in absolute CBF values ranging between 10 and 20%.

[¹⁵O]-H₂O-PET using ketamine-medetomidine anesthesia confirmed a significant acute difference in hemispheric CBF although much smaller than for the ASL perfusion measurements under isoflurane anesthesia. On the other hand, we did not observe differences in basal perfusion levels under α -chloralose/urethane anesthesia which appears contradictory.

This apparent discrepancy in initial CBF drop could not be explained by differences in physiological conditions as respiration rate and body temperature were similar between MRI scans sessions under isoflurane anesthesia (all time points) and under urethane/ α -chloralose (see supplementary Table 1). The isoflurane level of about 1.4% did cause on average a lower heart rate versus the urethane/ α -chloralose anesthesia (about 460 vs. 570 bpm, respectively (see supplementary Table 1).

A more plausible explanation can be found in the differential impact of these anesthetics on CBF. Isoflurane is a well-known potent vasodilator resulting in typically high-flow values compared to other anesthetics such as ketamine/xylazine.^{28,29} Similarly,

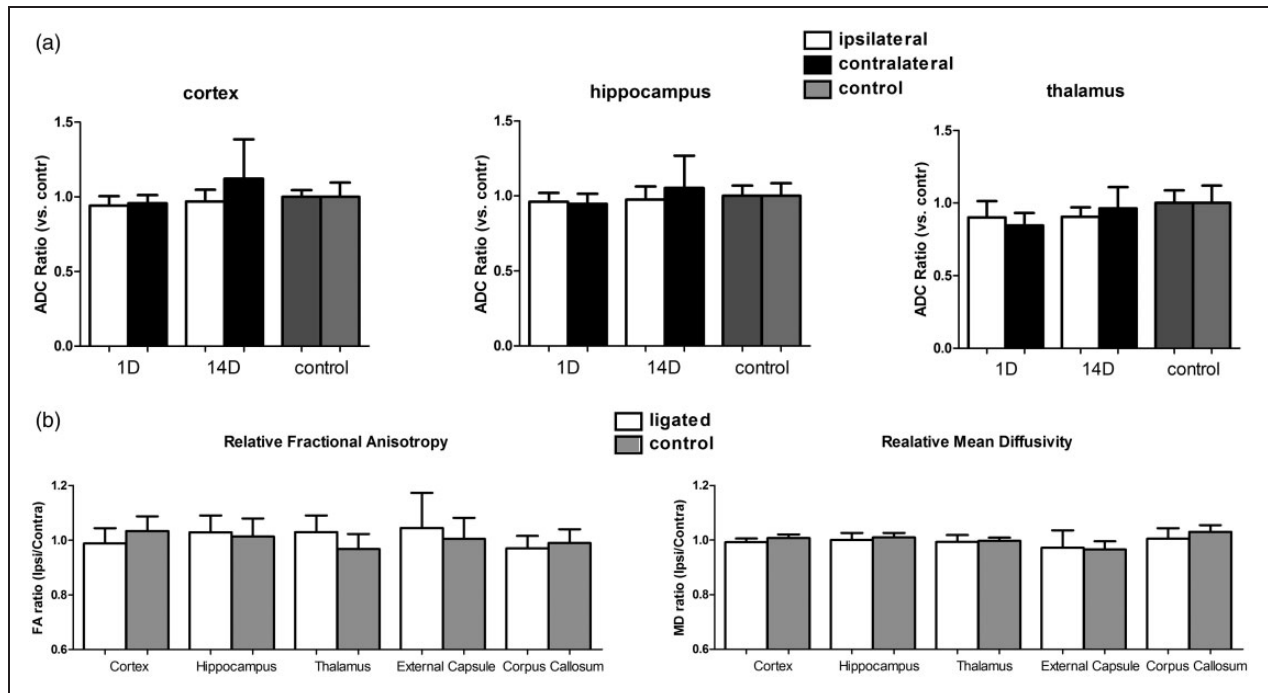


Figure 5. (a) Ipsi- and contralateral apparent diffusion constant (ADC) relative to the average ADC in control mice as calculated from DWI at 1 day and 2 weeks following permanent unilateral ligation of the CCA. No significant ADC changes were observed in all examined brain regions. (average \pm SD shown). (b) Fractional anisotropy (FA) and mean diffusivity ratio of the ipsi- to contralateral hemisphere as calculated from diffusion tensor imaging at 1 year following permanent unilateral ligation of the CCA. No significant FA and MD changes were observed in all examined brain regions. (average \pm SD shown). For precise animal numbers, please refer to supplemental Table 2.

exposing the mice to 5% CO₂ might not result in a substantial increase in CBF, as suggested by our preliminary experiments, due to the strong baseline vasodilation (although this effect may be dependent on the level of isoflurane anesthesia during baseline). Free breathing conditions during anesthesia may themselves cause hypercapnia, but this was not the case in our experiments with similar respiration rates during free breathing and normoventilation. The impact of the different anesthetics is also reflected in the considerably lower heart rate under the ketamine/medetomidine anesthesia (see supplementary Table 1). Medetomidine causes cardiovascular depression (reduced heart rate, hypotension) while this is much less the case during isoflurane or α -chloralose/urethane anesthesia.³⁰ This is also in agreement with our observation that a hypercapnic challenge under α -chloralose/urethane anesthesia, which increases base CBF,¹⁷ was able to demonstrate the compromised perfusion. Apart from the effect on vascular reactivity, the use of different anesthetics also affects other components of the neurovascular coupling being systemic physiology, vasoactive signal transmission and neural activity as reviewed by Masamoto and Kanno.³¹ Finally, perfusion levels are correlated with arterial pCO₂ levels. Arterial blood sampling is however non-trivial in mice

and repeated blood sampling is best avoided. We have previously shown that arterial pCO₂ levels are correlated with expired CO₂ levels (Oosterlinck et al.¹⁷). The expired CO₂ levels under baseline ventilation (200 \pm 10 a.u.) would correspond to expired CO₂ of about 30 mmHg. These longitudinal changes could not be explained by variability in hypercapnic challenge as expired CO₂ levels were comparable at all time points during normoventilation and rose to equal levels. These expired CO₂ levels correspond according to previous work¹⁷ in C57Bl6 mice to arterial pCO₂ levels of about 30 and 48 mmHg for normo- and hypoventilation, respectively.

When inducing hypercapnia, through hypoventilation, under α -chloralose/urethane, cerebral perfusion levels increased significantly in the contralateral hemisphere. However, no response was observed in the ipsilateral hemisphere at one day post-surgery. An increase in CBF was noticed at the two weeks and one month time point, but it was markedly less pronounced in the ipsi- vs. contralateral hemisphere. At two weeks, CVR values were still reduced in thalamus and hippocampus in the ipsilateral hemisphere compared to the contralateral hemisphere. Moreover, a tendency towards reduced CVR values at one month was observed in all examined brain regions (cortex, hippocampus and thalamus).

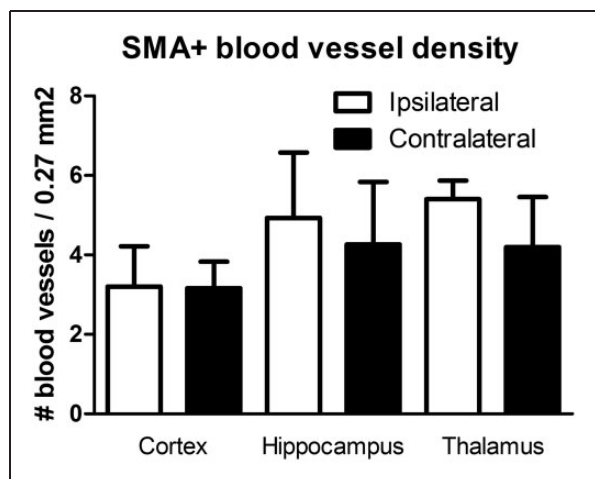


Figure 6. Quantification of alpha-SMA positive blood vessels in cortex, hippocampus and thalamus at 1 month post ligation. Although not significant, a trend towards a higher density was seen for the hippocampus and thalamus region (average \pm SD shown). For precise animal numbers, please refer to supplemental Table 2.

This suggests that, although a restoration in CVR is seen, the ability of vessels to dilate is still impaired at two weeks and likely at one month after CCA ligation. The partial recovery of CVR over time was previously explained by the enlargement of leptomeningeal collaterals 14 days after CCA occlusion and by the enlargement of the circle of Willis.^{8,32} Hecht et al. studied the vascular response capacity to an acetazolamide challenge using laser speckle imaging in young (12 weeks) and old (18 months) C57Bl6 mice up to 14 days after permanent right internal CAO.³³ In agreement with our data, they reported a functional compensation for the unilateral ligation after 14 days (and this in both young and old mice). Guo et al.³⁴ suggested capillary remodeling and collateral growth without angiogenesis after unilateral CCA ligation in mice.

To exclude any cytotoxic effect of the chronic hypoperfusion following permanent unilateral CCA ligation, cerebral diffusion parameters were evaluated at three different time points post-surgery (1 day, 7 days and 1 year). In stroke, the infarction core or ischemic lesions are often delineated based on a reduction in ADC values of more than 20% in the ipsilateral compared to the contralateral hemisphere.³⁵ For all examined time point and brain regions, our data did not show any significant changes in ADC, FA or MD values. The absence of lesions seen in diffusion images is in agreement with a previous report in which unilateral CCA ligation did not result in any ischemic lesions and that Cresyl violet-stained sections showed no cerebral infarction in mice with rCCA ligation seven days post-operation.¹⁶ Another study did, however, find

white matter damage in the corpus callosum determined from the fiber density of luxol-fast-blue-stained sections.²⁷ These latter findings can perhaps be attributed to a basal collateral flow that maintains perfusion in the ipsilateral hemisphere. In patients with unilateral carotid artery occlusion, the circle of Willis is considered as the primary collateral circulation. When this compensation is insufficient, secondary collaterals are recruited, such as the ophthalmic artery or leptomeningeal vessel.³⁶ Furthermore, pial collaterals, if well developed, might allow protracted tissue survival in the event of a proximal occlusion of a large intracranial blood vessel.³⁷ However, in mice, native pial collateral circulation varies largely between different genetic strains.³⁸ This variability emphasizes the need for non-invasive evaluation of the CBF for individual evaluation and to exclude the possibility that oligemia differently affects CBF in different genetic strains.

A previous report on right CCA ligation showed metabolic deficits with FDG-PET under chlorohydrate anesthesia in the ipsilateral parietal cortex of 14-month-old C57Bl6 mice two months after permanent unilateral ligation.¹⁶ In contrast, our results cannot confirm any short or long-term metabolic defects in this model in young mice under ketamine/medetomidine anesthesia.

Over the years, many animal models have been developed to mimic stroke in rodents with the tMCAO model being by far the most frequently used.³⁹ Inherent to this model, however, is the permanent unilateral ligation of the CCA, making the ipsilateral flow dependent on the collateral circulation. It has been reported that unilateral ligation of the CCA in the perinatal period (P12) leads to stroke lesion development in CD1 mice without applying supplementary hypoxia or pharmacological agents.⁴⁰ In this context, it is indispensable to gain in-depth information on the effect of such a ligation on the organization and function of the cerebrovascular network in order to correctly interpret possible effects of novel therapeutic agents. The results reported here are relevant to studies focusing on (re)perfusion of the penumbra area in stroke animals because a vascular response elicited by a permanent ligation of the carotid artery might affect the recovery seen in stroke animals that would be reduced in case of a non-ligated carotid artery.

In general, different protective mechanisms exist to counteract possible neuronal damage resulting from reduction in CBF and related hypoxic conditions. Local tissue perfusion can be increased by nitric oxide-mediated vasodilation and growth of new blood vessels (angiogenesis).⁴¹ At the cellular level, hypoxia-induced neuroprotective factors such as erythropoietin or vascular endothelial growth factor (VEGF) enhance survival of neuronal cells.⁴² The involvement of these factors under chronic hypoperfusion without the

presence of an acute ischemic lesion is, however, largely unknown. Multi-vessel occlusion models in rats have demonstrated processes of adaptation and compensation in the form of increased arteriogenesis and VEGF levels, counteracting the initially induced metabolic and functional deteriorations.⁴³ In mice, CBF and ATP metabolism recovered partially from an initially drastic reduction (to about 30% of basic values) after a step-wise bilateral CCAO.⁷ Altogether, many of these aspects discussed above may be activated or present upon permanent unilateral CCA ligation. As this ligation is present in some of the most frequently used stroke models and corresponding sham-operated control animals, it is of utmost importance to thoroughly screen stroke models for any of these effects. The data and methodology discussed in this paper provide a non-invasive and reproducible way to do so.

In contradiction to a recent study²⁵ on the bilateral stenosis model reporting considerable variability in the acute and long-term perfusion levels, our data show a very reproducible timeline in the perfusion changes after unilateral ligation. This is particularly striking since both studies were performed in the same mouse strain and at similar ages (8 vs. 10 weeks). However, these differences can be attributed to the different experimental approach used in both studies. In contrast to the complete ligation model used in our study, the study by Fuchtemeier et al.²⁵ used the placement of microcoils on the carotid arteries to mimic stenosis. Possible variability in the blood flow through these microcoils might increase the variability seen in the perfusion values.

Limitations of our study are that experiments were performed under hyperoxic conditions (either 100% or 47% O₂) and that the urethane/ α -chloralose anesthesia does not allow for a longitudinal study.

This study aimed at providing a methodological basis which can act as a starting point to further study the precise underlying mechanisms of the vascular remodeling seen following chronic hypoperfusion. The use of transgenic mouse strains in which angiogenesis is compromised would be a possible approach. Furthermore, the use of the same anesthetics in different approaches (free breathing vs. ventilated animals) is advisable to provide a better comparison of the results. The methodology described in this study would be suited to monitor short and long-term perfusion and vascular changes in ischemic stroke models such as the transient cerebral artery occlusion model. The model used in this study is a commonly used sham condition for tMCAO. The results described here can hold valuable information regarding correct interpretation of the vascular remodeling seen following ischemic stroke. Furthermore, the availability of different KO-strains such as mice lacking oxygen sensors in the brain⁴⁴ offer great potential to further

unravel the molecular mechanisms underlying the changes reported here.

We conclude that ASL-based perfusion MRI and MR angiography can be used to characterize both the acute and chronic vascular effects resulting from unilateral permanent CCA occlusion in mice. We further show that remodeling of the acute effects is sufficient for full recovery of hemispheric perfusion capabilities without metabolic or white matter changes but with long-term alterations in arterial tortuosity. These results are relevant to both studies of ischemic stroke and cognitive decline associated with vascular aspects.

Funding

The author(s) disclosed receipt of the following financial support for the research, authorship, and/or publication of this article: We gratefully acknowledge the following funding sources: The European Commission supported the INMiND project (FP7, Health-F2-2011-278850) and the Marie Curie training network EC-FP7-MC-ITN TransAct (316679). The Flemish government supported the IWT MIRIAD (SBO 130065) project and the FWO R-4894 project. The University of Leuven supports the Program Financing IMIR (10/017). CC and AB are postdoctoral Research Fellows of the FWO. KG is a PhD fellow of the FWO. KVL is a Senior Clinical Researcher of the FWO. TD has received funding from FWO for the KaN 1.5.220.13N.

Acknowledgements

We would like to thank Ann Van Santvoort for her excellent assistance in the animal work and Dr S. Fieuws for advice and helpful discussions regarding the statistical methodology.

Declaration of conflicting interests

The author(s) declared no potential conflicts of interest with respect to the research, authorship, and/or publication of this article.

Authors' contribution

All listed authors declare that they contributed to: The conception and design of this study, acquisition of data, analysis and interpretation of data: Tom Struys, Kristof Govaerts, Wouter Oosterlinck, Cindy Casteels, Annelies Bronckaers, Michel Koole, Uwe Himmelreich, Tom Dresselaers
Drafting/revising the manuscript: All listed authors
Final approval of the current version: All listed authors.

Supplementary material

Supplementary material for this paper can be found at <http://jcbfm.sagepub.com/content/by/supplemental-data>

References

1. Bokkers RP, Hernandez DA, Merino JG, et al. Whole-brain arterial spin labeling perfusion MRI in patients with acute stroke. *Stroke* 2012; 43: 1290–1294.

2. Scherr M, Trinka E, Mc Coy M, et al. Cerebral hypoperfusion during carotid artery stenosis can lead to cognitive deficits that may be independent of white matter lesion load. *Curr Neurovasc Res* 2012; 9: 193–199.
3. Hagendorff A, Klemm E, Bangard M, et al. Case report: regional cerebral hypoperfusion induced by ventricular tachycardia – short-term hippocampal hypoperfusion and its potential relationship to selective neuronal damage. *J Interv Cardiac Electrophysiol* 2001; 5: 435–441.
4. Leenders KL, Perani D, Lammertsma AA, et al. Cerebral blood flow, blood volume and oxygen utilization. Normal values and effect of age. *Brain* 1990; 113(Pt 1): 27–47.
5. de la Torre JC. Critically attained threshold of cerebral hypoperfusion: the CATCH hypothesis of Alzheimer's pathogenesis. *Neurobiol Aging* 2000; 21: 331–342.
6. Shibata M, Ohtani R, Ihara M, et al. White matter lesions and glial activation in a novel mouse model of chronic cerebral hypoperfusion. *Stroke* 2004; 35: 2598–2603.
7. Plaschke K, Sommer C, Schroeck H, et al. A mouse model of cerebral oligemia: relation to brain histopathology, cerebral blood flow, and energy state. *Exp Brain Res* 2005; 162: 324–331.
8. Kitagawa K, Yagita Y, Sasaki T, et al. Chronic mild reduction of cerebral perfusion pressure induces ischemic tolerance in focal cerebral ischemia. *Stroke* 2005; 36: 2270–2274.
9. Hara H, Huang PL, Panahian N, et al. Reduced brain edema and infarction volume in mice lacking the neuronal isoform of nitric oxide synthase after transient MCA occlusion. *J Cereb Blood Flow Metab* 1996; 16: 605–611.
10. Ito Y, Tsurushima H, Sato M, et al. Angiogenesis therapy for brain infarction using a slow-releasing drug delivery system for fibroblast growth factor 2. *Biochem Biophys Res Commun* 2013; 432: 182–187.
11. Jiang WL, Zhang SP, Zhu HB, et al. Effect of 8-O-acetyl shanzhiside methylester increases angiogenesis and improves functional recovery after stroke. *Basic Clin Pharmacol Toxicol* 2011; 108: 21–27.
12. Hoehn M, Nicolay K, Franke C, et al. Application of magnetic resonance to animal models of cerebral ischemia. *J Magn Reson Imaging* 2001; 14: 491–509.
13. Pham M, Helluy X, Braeuninger S, et al. Outcome of experimental stroke in C57Bl/6 and Sv/129 mice assessed by multimodal ultra-high field MRI. *Exp Transl Stroke Med* 2010; 2: 6.
14. Fraisl P, Aragones J and Carmeliet P. Inhibition of oxygen sensors as a therapeutic strategy for ischaemic and inflammatory disease. *Nature Reviews Drug Discov* 2009; 8: 139–152.
15. Elali A, Theriault P, Prefontaine P, et al. Mild chronic cerebral hypoperfusion induces neurovascular dysfunction, triggering peripheral beta-amyloid brain entry and aggregation. *Acta Neuropathol Commun* 2013; 1: 75.
16. Lee JS, Im DS, An YS, et al. Chronic cerebral hypoperfusion in a mouse model of Alzheimer's disease: an additional contributing factor of cognitive impairment. *Neurosci Lett* 2011; 489: 84–88.
17. Oosterlinck WW, Dresselaers T, Geldhof V, et al. Response of mouse brain perfusion to hypo- and hyper-ventilation measured by arterial spin labeling. *Magn Reson Med* 2011; 66: 802–811.
18. Kwong KK, Chesler DA, Weisskoff RM, et al. MR perfusion studies with T1-weighted echo planar imaging. *Magn Reson Med* 1995; 34: 878–887.
19. Kim SG and Tsekos NV. Perfusion imaging by a flow-sensitive alternating inversion recovery (FAIR) technique: application to functional brain imaging. *Magn Reson Med* 1997; 37: 425–435.
20. Kober F, Iltis I, Izquierdo M, et al. High-resolution myocardial perfusion mapping in small animals in vivo by spin-labeling gradient-echo imaging. *Magn Reson Med* 2004; 51: 62–67.
21. Likar B, Viergever MA and Pernus F. Retrospective correction of MR intensity inhomogeneity by information minimization. *IEEE Trans Med Imaging* 2001; 20: 1398–1410.
22. Bullitt E, Gerig G, Pizer SM, et al. Measuring tortuosity of the intracerebral vasculature from MRA images. *IEEE Trans Med Imaging* 2003; 22: 1163–1171.
23. Fox PT and Raichle ME. Focal physiological uncoupling of cerebral blood flow and oxidative metabolism during somatosensory stimulation in human subjects. *Proc Natl Acad Sci USA* 1986; 83: 1140–1144.
24. Soria G, Tudela R, Marquez-Martin A, et al. The ins and outs of the BCCAO model for chronic hypoperfusion: a multimodal and longitudinal MRI approach. *Plos One* 2013; 8: e74631.
25. Fuchtemeier M, Brinckmann MP, Foddiss M, et al. Vascular change and opposing effects of the angiotensin type 2 receptor in a mouse model of vascular cognitive impairment. *J Cereb Blood Flow Metab* 2014; 35: 476–484.
26. Holland PR, Bastin ME, Jansen MA, et al. MRI is a sensitive marker of subtle white matter pathology in hypoperfused mice. *Neurobiology Aging* 2011; 32: 2325 e1–6.
27. Yoshizaki K, Adachi K, Kataoka S, et al. Chronic cerebral hypoperfusion induced by right unilateral common carotid artery occlusion causes delayed white matter lesions and cognitive impairment in adult mice. *Exp Neurol* 2008; 210: 585–591.
28. Hendrich KS, Kochanek PM, Melick JA, et al. Cerebral perfusion during anesthesia with fentanyl, isoflurane, or pentobarbital in normal rats studied by arterial spin-labeled MRI. *Magn Reson Med* 2001; 46: 202–206.
29. Lei H, Grinberg O, Nwaigwe CI, et al. The effects of ketamine-xylazine anesthesia on cerebral blood flow and oxygenation observed using nuclear magnetic resonance perfusion imaging and electron paramagnetic resonance oximetry. *Brain Res* 2001; 913: 174–179.
30. Tremoleda JL, Kerton A and Gsell W. Anaesthesia and physiological monitoring during in vivo imaging of laboratory rodents: considerations on experimental outcomes and animal welfare. *EJNMMI Res* 2012; 2: 44.
31. Masamoto K and Kanno I. Anesthesia and the quantitative evaluation of neurovascular coupling. *J Cereb Blood Flow Metab* 2012; 32: 1233–1247.

32. Todo K, Kitagawa K, Sasaki T, et al. Granulocyte-macrophage colony-stimulating factor enhances leptomeningeal collateral growth induced by common carotid artery occlusion. *Stroke* 2008; 39: 1875–1882.
33. Hecht N, He J, Kremenetskaia I, et al. Cerebral hemodynamic reserve and vascular remodeling in C57/BL6 mice are influenced by age. *Stroke* 2012; 43: 3052–3062.
34. Guo H, Itoh Y, Toriumi H, et al. Capillary remodeling and collateral growth without angiogenesis after unilateral common carotid artery occlusion in mice. *Microcirculation* 2011; 18: 221–227.
35. van Dorsten FA, Hata R, Maeda K, et al. Diffusion- and perfusion-weighted MR imaging of transient focal cerebral ischaemia in mice. *NMR Biomed* 1999; 12: 525–534.
36. Hofmeijer J, Klijn CJ, Kappelle LJ, et al. Collateral circulation via the ophthalmic artery or leptomeningeal vessels is associated with impaired cerebral vasoreactivity in patients with symptomatic carotid artery occlusion. *Cerebrovasc Dis* 2002; 14: 22–26.
37. Shuaib A, Butcher K, Mohammad AA, et al. Collateral blood vessels in acute ischaemic stroke: a potential therapeutic target. *Lancet Neurol* 2011; 10: 909–921.
38. Zhang H, Prabhakar P, Sealock R and Faber JE. Wide genetic variation in the native pial collateral circulation is a major determinant of variation in severity of stroke. *J Cereb Blood Flow Metab* 2010; 30: 923–934.
39. Liu F and McCullough LD. Middle cerebral artery occlusion model in rodents: methods and potential pitfalls. *J Biomed Biotechnol* 2011; 2011: 464701.
40. Comi AM, Johnston MV and Wilson MA. Immature mouse unilateral carotid ligation model of stroke. *J Child Neurol* 2005; 20: 980–983.
41. Marti HH. Angiogenesis – a self-adapting principle in hypoxia. *Exs* 2005; 94: 163–180.
42. Wang Y, Kilic E, Kilic U, et al. VEGF overexpression induces post-ischaemic neuroprotection, but facilitates haemodynamic steal phenomena. *Brain* 2005; 128(Pt 1): 52–63.
43. Plaschke K, Sommer C, Fahrner A, et al. Pronounced arterial collateralization was induced after permanent rat cerebral four-vessel occlusion. Relation to neuropathology and capillary ultrastructure. *J Neural Transm* 2003; 110: 719–732.
44. Quaegebeur A, Segura I, Schmieder R, et al. Deletion or inhibition of the oxygen sensor PHD1 protects against ischemic stroke via reprogramming of neuronal metabolism. *Cell Metab* 2016; 9: 280–281.